Research Article | Vol. 25, No. 6 | 20 Mar 2017 | OPTICS EXPRESS 6561

Optics EXPRESS

Ge-rich graded-index $Si_{1-x}Ge_x$ waveguides with broadband tight mode confinement and flat anomalous dispersion for nonlinear mid-infrared photonics

J. M. RAMIREZ,[1,*] V. VAKARIN,[1] J. FRIGERIO,[2] P. CHAISAKUL,[1] D. CHRASTINA,[2] X. LE ROUX,[1] A. BALLABIO,[2] L. VIVIEN,[1] G. ISELLA,[2] AND D. MARRIS-MORINI[1]

[1]*Centre de Nanosciences et de Nanotechnologies, Université Paris Sud, CNRS, Université Paris Saclay, 91405 Orsay, France*
[2]*L-NESS, Dipartimento di Fisica, Politecnico di Milano, Polo di Como, Via Anzani 42, 22100 Como, Italy*
**joan-manel.ramirez@u-psud.fr*
http://silicon-photonics.ief.u-psud.fr/

Abstract: This work explores the use of Ge-rich graded-index $Si_{1-x}Ge_x$ rib waveguides as building blocks to develop integrated nonlinear optical devices for broadband operation in the mid-IR. The vertical Ge gradient concentration in the waveguide core renders unique properties to the guided optical mode, providing tight mode confinement over a broadband mid-IR wavelength range from λ = 3 μm to 8 μm. Additionally, the gradual vertical confinement pulls the optical mode upwards in the waveguide core, overlapping with the Ge-rich area where the nonlinear refractive index is larger. Moreover, the Ge-rich graded-index $Si_{1-x}Ge_x$ waveguides allow efficient tailoring of the chromatic dispersion curves, achieving flat anomalous dispersion for the quasi-TM optical mode with $D \leq 14$ ps/nm/km over a ~1.4 octave span while retaining an optimum third-order nonlinear parameter, γ_{eff}. These results confirm the potential of Ge-rich graded-index $Si_{1-x}Ge_x$ waveguides as an attractive platform to develop mid-IR nonlinear approaches requiring broadband dispersion engineering.

OCIS codes: (190.4390) Nonlinear optics, integrated optics; (190.3270) Kerr effect; (130.2035) Dispersion compensation devices.

References and links

1. R. Soref, "Mid-infrared photonics in silicon and germanium," Nat. Photonics **4**(8), 495–497 (2010).
2. Editorial "Extending opportunities," Nat. Photonics **6**(7), 407 (2012).
3. J. Faist, F. Capasso, D. L. Sivco, C. Sirtori, A. L. Hutchinson, and A. Y. Cho, "Quantum cascade laser," Science **264**(5158), 553–556 (1994).
4. B. Kuyken, X. Liu, R. M. Osgood, Jr., R. Baets, G. Roelkens, and W. M. Green, "Mid-infrared to telecom-band supercontinuum generation in highly nonlinear silicon-on-insulator wire waveguides," Opt. Express **19**(21), 20172–20181 (2011).
5. A. Spott, Y. Liu, T. Baehr-Jones, R. R. Ilic, and M. Hochberg, "Silicon Waveguides and Ring Resonators at 5.5 μm," Appl. Phys. Lett. **97**, 213501 (2010).
6. S. Khan, J. Chiles, J. Ma, and S. Fathpour, "Silicon-on-nitride waveguides for mid-and near-infrared integrated photonics," Appl. Phys. Lett. **102**(12), 121104 (2013).
7. J. S. Penadés, C. Alonso-Ramos, A. Z. Khokhar, M. Nedeljkovic, L. A. Boodhoo, A. Ortega-Moñux, I. Molina-Fernández, P. Cheben, and G. Z. Mashanovich, "Suspended SOI waveguide with sub-wavelength grating cladding for mid-infrared," Opt. Lett. **39**(19), 5661–5664 (2014).
8. H. Lin, L. Li, Y. Zou, S. Danto, J. D. Musgraves, K. Richardson, S. Kozacik, M. Murakowski, D. Prather, P. T. Lin, V. Singh, A. Agarwal, L. C. Kimerling, and J. Hu, "Demonstration of high-Q mid-infrared chalcogenide glass-on-silicon resonators," Opt. Lett. **38**(9), 1470–1472 (2013).
9. Y. C. Chang, P. Wägli, V. Paeder, A. Homsy, L. Hvozdara, P. van der Wal, J. Di Francesco, N. F. de Rooij, and H. P. Herzig, "Cocaine detection by a mid-infrared waveguide integrated with a microfluidic chip," Lab Chip **12**(17), 3020–3023 (2012).

#285353 https://doi.org/10.1364/OE.25.006561
Journal © 2017 Received 20 Jan 2017; revised 8 Mar 2017; accepted 8 Mar 2017; published 13 Mar 2017

Optics EXPRESS

10. A. Malik, M. Muneeb, S. Pathak, Y. Shimura, J. Van Campenhout, R. Loo, and G. Roelkens, "Germanium-on-silicon mid-infrared arrayed waveguide grating multiplexers," IEEE Photonics Technol. Lett. **25**(18), 1805–1808 (2013).
11. A. Malik, S. Dwivedi, L. Van Landschoot, M. Muneeb, Y. Shimura, G. Lepage, J. Van Campenhout, W. Vanherle, T. Van Opstal, R. Loo, and G. Roelkens, "Ge-on-Si and Ge-on-SOI thermo-optic phase shifters for the mid-infrared," Opt. Express **22**(23), 28479–28488 (2014).
12. F. De Leonardis, B. Troia, and V. M. Passaro, "Mid-IR optical and nonlinear properties of germanium on silicon optical waveguides," J. Lightwave Technol. **32**(22), 3747–3757 (2014).
13. P. Barritault, M. Brun, P. Labeye, O. Lartigue, J. M. Hartmann, and S. Nicoletti, "Mlines characterization of the refractive index profile of SiGe gradient waveguides at 2.15 µm," Opt. Express **21**(9), 11506–11515 (2013).
14. M. Brun, P. Labeye, G. Grand, J. M. Hartmann, F. Boulila, M. Carras, and S. Nicoletti, "Low loss SiGe graded index waveguides for mid-IR applications," Opt. Express **22**(1), 508–518 (2014).
15. J. M. Ramirez, V. Vakarin, C. Gilles, J. Frigerio, A. Ballabio, P. Chaisakul, X. L. Roux, C. Alonso-Ramos, G. Maisons, L. Vivien, M. Carras, G. Isella, and D. Marris-Morini, "Low-loss Ge-rich Si0.2Ge0.8 waveguides for mid-infrared photonics," Opt. Lett. **42**(1), 105–108 (2017).
16. F. De Leonardis, B. Troia, R. A. Soref, and V. M. N. Passaro, "Dispersion of nonresonant third-order nonlinearities in GeSiSn ternary alloys," Sci. Rep. **6**(1), 32622 (2016).
17. P. Moontragoon, R. A. Soref, and Z. Ikonic, "The direct and indirect bandgaps of unstrained $Si_xGe_{1-x-y}Sn_y$ and their photonic device applications," J. Appl. Phys. **112**(7), 073106 (2012).
18. L. Zhang, A. M. Agarwal, L. C. Kimerling, and J. Michel, "Nonlinear Group IV photonics based on silicon and germanium: from near-infrared to mid-infrared," Nanophotonics **3**(4–5), 247–268 (2014).
19. B. Tatian, "Fitting refractive-index data with the Sellmeier dispersion formula," Appl. Opt. **23**(24), 4477–4485 (1984).
20. N. Singh, D. D. Hudson, and B. J. Eggleton, "Silicon-on-sapphire pillar waveguides for Mid-IR supercontinuum generation," Opt. Express **23**(13), 17345–17354 (2015).
21. L. Zhang, Q. Lin, Y. Yue, Y. Yan, R. G. Beausoleil, and A. E. Willner, "Silicon waveguide with four zero-dispersion wavelengths and its application in on-chip octave-spanning supercontinuum generation," Opt. Express **20**(2), 1685–1690 (2012).
22. N. Singh, D. D. Hudson, Y. Yu, C. Grillet, S. D. Jackson, A. Casas-Bedoya, A. Read, P. Atanackovic, S. G. Duvall, S. Palomba, B. Luther-Davies, S. Madden, D. J. Moss, and B. J. Eggleton, "Midinfrared supercontinuum generation from 2 to 6 µm in a silicon nanowire," Optica **2**(9), 797–802 (2015).
23. A. Kordts, M. H. P. Pfeiffer, H. Guo, V. Brasch, and T. J. Kippenberg, "Higher order mode suppression in high-Q anomalous dispersion SiN microresonators for temporal dissipative Kerr soliton formation," Opt. Lett. **41**(3), 452–455 (2016).
24. N. K. Hon, R. Soref, and B. Jalali, "The third-order nonlinear optical coefficients of Si, Ge, and $Si_{1-x}Ge_x$ in the midwave and longwave infrared," J. Appl. Phys. **110**(1), 011301 (2011).
25. M. Foster, K. Moll, and A. Gaeta, "Optimal waveguide dimensions for nonlinear interactions," Opt. Express **12**(13), 2880–2887 (2004).
26. L. Carletti, M. Sinobad, P. Ma, Y. Yu, D. Allioux, R. Orobtchouk, M. Brun, S. Ortiz, P. Labeye, J. M. Hartmann, S. Nicoletti, S. Madden, B. Luther-Davies, D. J. Moss, C. Monat, and C. Grillet, "Mid-Infrared nonlinear optical response of Si-Ge waveguides with ultra-short optical pulses," Opt. Express **23**(25), 32202–32214 (2015).

1. Introduction

Mid-infrared (mid-IR) photonics has been often postulated as an interesting discipline meant to lead to key advances in several fields covering chemical and biological sensing, thermal imaging, early medical diagnosis or secure communications, among others [1, 2]. Renewed interest has been recently triggered, partially motivated by the advent of quantum cascade lasers (QCLs) that provide compact and tunable mid-IR laser sources with high output powers [3]. Such great potential has stimulated research towards the implementation of compact and low-cost mid-IR integrated photonic chips, taking advantage of a mature silicon technology. In that regard, one of the first platforms to be explored in the mid-IR range was Si-on-insulator (SOI), encouraged by the outstanding performance offered by the SOI platform at telecom wavelengths [4]. Nevertheless, the early absorption of the buried oxide around of λ = 3.6 µm limits its operation to the lowest spectral region of the mid-IR band. Other platforms such as silicon-on-sapphire (SOS) or silicon-on-silicon nitride (SON) were able to extend the cut-off wavelength up to 6 µm [5, 6], whereas silicon-on-porous silicon (SiPSi), suspended silicon schemes, or the implementation of hybrid approaches permitted the Si transparency window to be fully exploited until 8 µm [7, 8]. Alternatively, the use of Ge-on-Si platforms for mid-IR integrated photonics allowed the wavelength range to be further extended up to 14 µm while using a fully monolithic and robust approach [9–11]. Furthermore, the

Optics EXPRESS

implementation of Ge-based optical systems provides good prospects to develop nonlinear mid-IR optical devices, owing to its larger nonlinear refractive index than Si and the suppression of two-photon absorption in Ge for $\lambda > 3.17$ μm [12]. Later on, $Si_{1-x}Ge_x$ alloys gained attention due to their ability to fine-tune the refractive index and bandgap at will, being able to provide complex graded refractive index profiles to efficiently accommodate the guided optical mode [13]. As a result, competitive propagation losses as low as 1 dB/cm for λ = 4.5 μm and 2 dB/cm for λ = 7.4 μm were obtained by ramping the Ge concentration in the $Si_{1-x}Ge_x$ alloy up to ≈40% [14]. More recently, low-loss Ge-rich $Si_{1-x}Ge_x$ waveguides with a top Ge concentration up to 80% were also demonstrated at λ = 4.6 μm [15]. As Ge transparency extends up to 15 μm, the Ge-rich $Si_{1-x}Ge_x$ platform presents strong advantages in terms of maximum wavelength of operation. In addition, the strong Kerr effect of Ge opens a new route towards the implementation of efficient mid-IR non-linear devices based on these structures [16–18].

Thus, in this paper the potential of this approach as an enabling platform to develop broadband non-linear mid-IR devices such as supercontinuum light sources has been assessed. First, a modal and dispersive analysis of mid-IR Ge-rich graded-index $Si_{1-x}Ge_x$ rib waveguides has been performed, in order to find the best waveguide geometry that yields tight mode confinement and flat anomalous dispersion over a broadband mid-IR wavelength range (from λ = 3 μm to λ = 8 μm). Such wavelength span was determined, in the short wavelength regime, around the onset of two-photon absorption in Ge (i. e. λ ~3.2 μm). In the upper wavelength regime, the longest operation wavelength was obtained according to the maximum value providing anomalous dispersion condition in both polarizations, which is around of λ ~8 μm for the optimized design. Finally, the third order nonlinear parameter (γ_{eff}) has been evaluated over such a broadband mid-IR wavelength reach (~1.4 octave span), showing the suitability of this platform for mid-IR nonlinear optics.

2. Design rules for Ge-rich graded-index $Si_{1-x}Ge_x$ mid-IR rib waveguides

Simulations of mid-IR waveguides were done using a finite-difference method (FDM) mode solver, taking into account the refractive index wavelength dependence of Si and Ge [15, 19]. The proposed waveguide consists of a graded-index $Si_{1-x}Ge_x$ waveguide core region (h_{core}) from Si to Ge on a Si substrate, as shown in Fig. 1 (a). The graded refractive index profile provided by the linear increase of the Ge concentration along the guiding core vertical direction was implemented using a linear relation between the Si and Ge refractive index values, according to the Ge concentration (x) of the $Si_{1-x}Ge_x$ alloy. A representative example of the obtained refractive index profile in the waveguide core region for λ = 3 μm is displayed in Fig. 1(b), with a grading rate of ≈16.6% /μm (h_{core} = 6 μm).

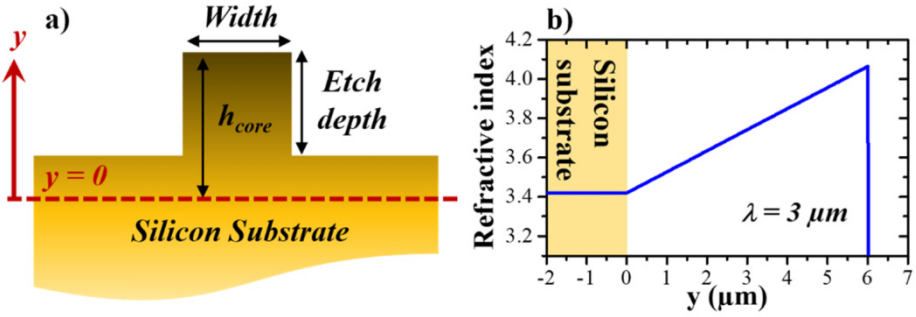

Fig. 1. a) Representative scheme of the graded-index $Si_{1-x}Ge_x$ waveguide cross-section. b) Calculated vertical refractive index profile of a graded-index $Si_{1-x}Ge_x$ waveguide (h_{core} = 6 μm and λ = 3 μm). y (μm) corresponds to the vertical position in the waveguide, being its origin located at the interface between the Si substrate and the graded-index $Si_{1-x}Ge_x$ waveguide, as marked with a horizontal dashed line in figure (a)).

Optics EXPRESS

A fundamental factor to consider when designing nonlinear waveguides is the optimum value of h_{core} yielding the best mode confinement in the mid-IR regime under study. Generally, small h_{core} values are desired since they provide steeper refractive index profiles and therefore tighter mode confinement in the guiding core. As an illustrative example, we may compare the modal effective area (A_{eff}) of the fundamental quasi-TM mode of a representative design using an h_{core} = 11 μm (similar to the one used in previous works, see ref. 15) with a design containing a reduced h_{core} = 6 μm. A moderate difference is observed at λ = 3 μm, being A_{eff}^{TM} (h_{core} = 6 μm) ≈4.4 μm^2 and A_{eff}^{TM} (h_{core} = 11 μm) ≈5.4 μm^2, which however becomes progressively larger for longer wavelengths up to a value of A_{eff}^{TM} (h_{core} = 6 μm) ≈10 μm^2 and A_{eff}^{TM} (h_{core} = 11 μm) ≈13 μm^2 at λ = 8 μm. On the other hand, an excessive reduction of the h_{core} will also compromise an efficient adaptation of the lattice parameter (from Si to Ge) with a subsequent increase of the threading dislocation density (TDD). Moreover, to better exploit the superior features of Ge over Si in the mid-IR, the propagating mode should overlap with the Ge-rich region of the waveguide core, which corresponds to its uppermost part. Thus, we used an h_{core} = 6 μm as yielded a good balance between tight mode confinement, good mode overlap with the Ge-rich region and an expected low dislocation density upon fabrication by state-of-the-art deposition techniques. In that regard, suitable techniques that have already provided notable results are reduced pressure chemical vapor deposition (RPCVD) or low energy plasma enhanced chemical vapor deposition (LEPECVD), among others [14, 15].

Similarly, the selection of the optimum waveguide width and etching depth values should also be carefully chosen. On the one hand, a small nonlinear modal effective area (A_{eff}^{NL}) is desired to boost the nonlinear phenomena. On the other hand, and since flat anomalous dispersion is required to fully exploit phase-matched nonlinear effects, waveguide dispersion engineering should be tackled. Finally, single mode operation is generally preferred to minimize power leakage due to mode cross-talk. In practice however, this condition is often relaxed in nonlinear optical devices showing a broadband anomalous regime [20–22]. In that case, single mode filtering regions have been proposed to address intermodal coupling in multimode structures and thus ensure propagation in the fundamental mode [23].

3. Dispersive properties and third order nonlinearities of Ge-rich graded-index $Si_{1-x}Ge_x$ mid-IR rib waveguides

The waveguide chromatic dispersion has been investigated as a function of the waveguide width and etching depth over a wavelength range of λ = 3-8 μm. Upper panels in Fig. 2(a), 2(b) and 2(c) show the dispersion (D) of the quasi-TE propagating mode for three representative wavelengths, i. e. at λ = 3 μm / 5.5 μm / 8 μm, and for a range of etching depths and waveguide widths that span from 1 to 5 μm (y-axis) and from 1 to 10 μm (x-axis), respectively. Multicolored areas represent designs with anomalous dispersion, whereas dark blue regions display geometries where normal dispersion was found. As seen, although multiple parameters provide anomalous dispersion, all of them lie outside the single mode domain, whose frontier is defined by a solid white line. Among them, a design with a width of 4 μm and an etching depth of 4 μm was chosen (marked by the grey dots) as it displayed broadband anomalous dispersion with values comprised within the low anomalous dispersion regime (D < 100 ps/nm/km). The calculated spectral dispersion characteristics of quasi-TE and quasi-TM polarizations have been compared in Fig. 2(d). As seen, both polarizations provide broadband anomalous dispersion over a 1.4 octave span, with the quasi-TM mode showing a flatter profile with a maximum value of ≈14 ps/nm/km for λ = 6 μm. The origin of such low dispersion characteristic compared to the quasi-TE mode is probably related to the enhanced influence of the vertical confinement the quasi-TM polarization is subjected to, hence benefiting from a stronger interaction with the vertical graded refractive index and therefore a better dispersion accommodation upon a wavelength variation.

Optics EXPRESS

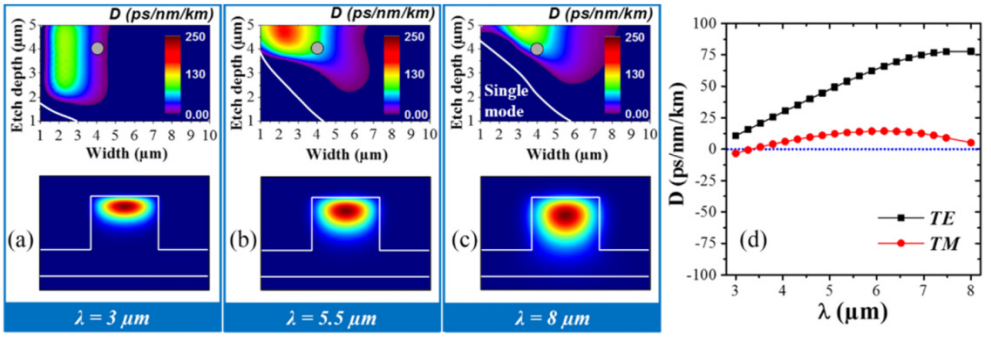

Fig. 2. Top panels in (a), (b) and (c) show the dispersion parameter (D) of the quasi-TE polarization mode (in multicolor scale) of a waveguide with h_{core} = 6 μm as a function of the etching depth and the waveguide width for λ = 3 μm / 5.5 μm / 8 μm. Multicolored areas correspond to positive (anomalous) dispersion. The grey dot indicates the selected waveguide parameters, with width = 4 μm and etching depth = 4 μm. Bottom panels in (a), (b) and (c) display the simulated optical propagation mode (quasi-TE) of the selected waveguide geometry for increasing λ, according to top panels. (d) Spectral evolution of the dispersion parameter of the quasi-TE (black squares) and quasi-TM (red dots) polarizations for the optimized waveguide design (h_{core} = 6 μm, width = 4 μm, etch depth = 4 μm).

Broadband phase-matched nonlinear mid-IR devices can thus be expected, providing strong light confinement of the optical modes. The bottom images in Fig. 2(a), 2(b) and 2(c) display the simulated mode profile of the dispersion engineered waveguide for λ = 3 μm / 5.5 μm / 8 μm. Remarkably, the propagating mode is localized entirely in the upper part of the waveguide, expanding towards the substrate for longer wavelengths. Such wavelength-dependent modal resizing is a unique feature of waveguides with graded-index guiding cores in the vertical direction, which are able to provide tight mode confinement over a broad wavelength range while retaining large cut-off wavelengths using a single waveguide geometry. Moreover the mode lies in the Ge-rich region of the waveguide, which is an advantage because of its large Kerr effect. Indeed, as Si and Ge are centro-symmetric materials, the advent of nonlinear properties is mainly governed by the third order nonlinearity ($\chi^{(3)}$), and particularly by the Kerr coefficient (n_2), whose values, extracted from [24] are reported in Fig. 3(a) for different Ge concentrations of the $Si_{1-x}Ge_x$ alloy and for different λ values. Noticeably, larger n_2 values are observed for high Ge concentrations. The gradual increase of the Ge concentration inside the waveguide core thus provides a gradient of the n_2 parameter along the vertical direction. This situation is depicted in Fig. 3(b), where the spatial distribution of $n_2(y)$ of a graded-index $Si_{1-x}Ge_x$ waveguide operating at λ = 3 μm has been represented in a color bar scale. Notably, a constant Kerr coefficient is observed all over the waveguide for Ge concentrations lower than 80% ($n_2 \approx 1 \times 10^{-17}$ m^2/W), whereas a prominent enhancement of up to one order of magnitude is obtained for larger Ge concentrations ($n_2 = 1 \times 10^{-16}$ m^2/W for pure Ge). Therefore, the graded-index $Si_{1-x}Ge_x$ platform provides an optimum spatial overlap between the calculated optical mode (concentric lines superimposed in Fig. 3(b)) and the highly nonlinear area in the waveguide core in a broadband mid-IR range.

Figure 3(c) compares the normalized TE mode profile, $|E_{||}|$ (left y-axis, in black) and the calculated n_2 (right y-axis, in red) along the waveguide vertical direction for λ = 3 μm (solid lines) and λ = 8 μm (dashed-dotted lines), respectively (extreme values). As seen, the increase of λ is expected to gradually attenuate the nonlinear response of the waveguide in three different manners: (i) by consistently decreasing the top value of the $n_2(y)$ curve by ~50% compared to the value at λ = 3 μm; (ii) by reducing the modal overlap with the highly nonlinear area in the waveguide (y > 4.8 μm) from 65% for λ = 3 μm down to 30% for λ = 8 μm, and (iii) by the continuous downwards modal expansion that takes place for larger

Optics EXPRESS

wavelengths, which increases A_{eff}^{NL}. This trend is better seen in Fig. 3(d), where the effective nonlinear parameter (γ_{eff}) of graded-index $Si_{1-x}Ge_x$ waveguides has been calculated (right *y*-axis scale) and compared with A_{eff}^{NL} (left *y*-axis scale), displaying opposite trends. The following expression has been used [25]:

$$\gamma_{eff}(\lambda) = 2\pi \iint_{Wg} n_2(x,y) \cdot S_z^2 \, dxdy \Big/ \lambda \left(\int_{-\infty}^{\infty} \int S_z dxdy \right)^2 \quad (1)$$

with $S_z = (E \times H^*)_z$ the longitudinal component of the Poynting vector and the interval *Wg* in the numerator the geometrical boundary limits of the waveguide cross-section. As expected, the graded-index $Si_{1-x}Ge_x$ waveguide with h_{core} = 6 µm, Width = 4 µm and *Etch depth* = 4 µm provides a maximum value of $\gamma_{eff} \approx 10$ $W^{-1}m^{-1}$ for both polarizations at λ = 3 µm, followed by a gradual decrease for larger wavelengths down to $\gamma \sim 0.6$ $W^{-1}m^{-1}$ for λ = 8 µm. Moreover, although the quasi-TE polarization displays slightly larger γ_{eff} values all over the studied wavelength range, the quasi-TM propagation mode offers also good γ_{eff} values with flatter chromatic dispersion characteristic (see Fig. 2(a)). Finally, the potential of such graded-index $Si_{1-x}Ge_x$ waveguides for mid-IR nonlinear optics was further corroborated by comparing these results with previously reported simulations on the mid-IR supercontinuum generation of step index Si-cladded $Si_{0.6}Ge_{0.4}$ waveguides [26]. In that work, a supercontinuum spanning from λ = 2.5 µm to 6 µm was predicted by pumping a 6 cm long waveguide with an ultra-fast pulsed laser (320 fs) at a wavelength of λ = 4 µm, assuming a $\gamma_{eff} \sim 1$ $W^{-1}m^{-1}$ (with $A_{eff}^{NL} \sim 10$ µm^2). In our case, since the calculated γ_{eff} parameter is five times higher at this wavelength (λ = 4 µm), the Kerr effect is expected to manifest over shorter waveguide lengths and at lower pump power. Moreover, the calculated Kerr effect at λ = 8 µm for graded-index $Si_{1-x}Ge_x$ waveguides is still comparable to the value reported in [23] at λ = 4 µm, suggesting that prominent third order nonlinearities may also be observed at longer wavelengths in this platform.

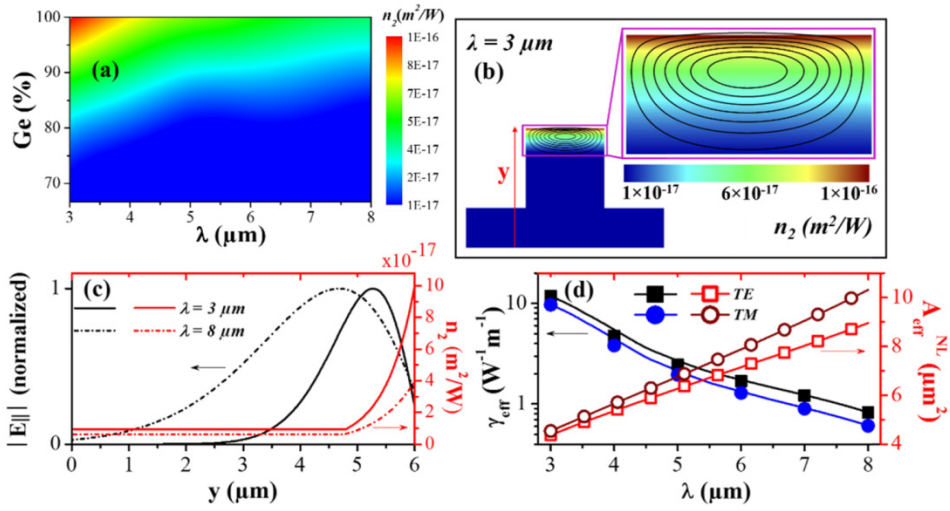

Fig. 3. (a) Color map of the calculated Kerr coefficient, n_2, extracted from [21], as a function of the Ge concentration and wavelength, λ. A constant value of $n_2 \approx 1 \times 10^{-17}$ m^2/W was obtained for the Ge concentrations not displayed (i. e. for Ge conc. < 65%). (b) Spatial distribution of n_2 in the waveguide, with the simulated modal intensity superimposed for λ = 3 µm (inner lines denote higher intensity). (c) Calculated quasi-TE mode profile ($|E_{||}|$, black curves, left y-axis) and n_2 (red curves, right y-axis) along the waveguide vertical direction for λ = 3 µm (solid lines) and λ = 8 µm (dashed dotted lines). (d) Calculated nonlinear parameter (γ_{eff}, filled data, left y-axis) and nonlinear modal effective area (A_{eff}^{NL}, empty data, right y-axis) of the quasi-TE (squares) and quasi-TM (circles) optical modes as a function of λ.

Optics EXPRESS

4. Conclusions

In this work, the potential of Ge-rich graded-index $Si_{1-x}Ge_x$ waveguides for broadband mid-IR nonlinear applications was studied over the wavelength range from λ = 3 μm to 8 μm. The best waveguide geometrical parameters yielding broadband tight mode confinement and flat anomalous dispersion were inspected, revealing a strong mode overlap with the Ge-rich area and a gradual wavelength-dependent size accommodation of the guided optical mode caused by the vertical Ge gradient concentration in the waveguide core. Additionally, broadband anomalous dispersion was engineered for both quasi-TE and quasi-TM fundamental optical modes, giving rise to a particularly flat profile for the quasi-TM polarization with values comprised between D = −3 ps/nm/km and 14 ps/nm/km. Finally, the spatial distribution map of the Kerr effect coefficient in dispersion engineered Ge-rich graded-index $Si_{1-x}Ge_x$ waveguides was calculated, allowing us to estimate the evolution of the effective nonlinear parameter (γ_{eff}) as a function of the propagating wavelength. Promising values were retrieved, with a maximum of γ_{eff} ~10 $W^{-1}m^{-1}$ for λ = 3 μm followed by a gradual decrease for longer wavelengths down to γ_{eff} ~0.6 $W^{-1}m^{-1}$ at λ = 8 μm, suggesting a promising performance for broadband supercontinuum generation.

Funding

European Research Council (ERC) under the European Union's Horizon 2020 research and innovation program (N°639107-INsPIRE).